Journal of Luminescence 213 (2019) 29–35

Contents lists available at ScienceDirect

Journal of Luminescence

journal homepage: www.elsevier.com/locate/jlumin

Photoluminescence and nonlinear transmission of Cu-doped CdSe quantum dots

A.M. Smirnov[a,b], A.D. Golinskaya[e,a], P.A. Kotin[c], S.G. Dorofeev[c], V.V. Palyulin[b,d], V.N. Mantsevich[b,e,*], V.S. Dneprovskii[b]

[a] Kotel'nikov Institute of RAS, Moscow, 125009, Russia
[b] Moscow State University, Faculty of Physics, Chair of Semiconductors and Cryoelectronics, Moscow, 119991, Russia
[c] Moscow State University, Faculty of Chemistry, Moscow, 119991, Russia
[d] Center for Computational and Data-intensive Science and Engineering, Skolkovo Institute of Science and Technology, Nobelya Ulitsa 3, Moscow, 121205, Russia
[e] Moscow State University, Faculty of Physics, Quantum Technology Center, Moscow, 119991, Russia

ARTICLE INFO

Keywords:
Nanoplatelets
Copper doped CdSe quantum dots
Photoluminescence
Pump-probe technique
Excitons scattering
Nonlinear optics

ABSTRACT

In this paper we investigate the photoluminescence (PL) properties and nonlinear transmission of Cu-doped CdSe colloidal quantum dots (QDs) under a nanosecond laser pulse excitation. We find a strong difference of the pump intensity dependent behavior between the basic exciton transition and Cu dopants associated PL. We also study the saturation of absorption in Cu-doped CdSe QDs. The role of a strong electron-phonon interaction in the PL properties and nonlinear transmission of colloidal Cu-doped CdSe QDs is explained. The presence of **biexciton PL** exciton-phonon interaction and its strong influence on the **basic exciton** PL and non-linear properties of Cu-doped colloidal CdSe QDs are proved by the simultaneous linear growth of basic excitons PL, the growth of the Stokes shift and significant decrease of absorption at the basic exciton transition wavelength with the increase of pump intensity.

1. Introduction

Colloidal semiconductor nanocrystals (QDs, nanoplatelets) form an appealing class of highly tunable materials with the wide range of potential applications [1–3]. In particular, by changing their size and the shape a substantial adjustment of the electronic structure becomes possible even without alteration of a chemical composition [4,5]. An insertion of luminescent dopant ions (Mn, Al, Ag, Au, Pb ions, etc.) into the semiconductor nanocrystals leads to the formation of additional energy states between the valence and conduction bands in semiconductor nanocrystal and changes the photophysical relaxation processes [6–15]. As a result, the dopant emission effects in the new optical properties whose nature changes depending on hosts and dopants used.

A substantial research interest is focused currently on the Cu-doped semiconductor nanocrystals which combine the unique luminescent properties of copper-doped semiconductors with the solubility and optoelectronic tunability of semiconductor nanocrystals [16]. The copper-doped nanocrystals possess a composition-tunable energy gap and display a very broad, tunable PL bands centered significantly lower than their band-gap energies [17–19]. This high tunability in combination with an extremely small overlap between their PL and absorption spectra, broad emission spectral window, minimum self-absorption, long lifetime of the excited state as well as thermal stability makes Cu-doped nanocrystals a promising candidate for numerous applications in spectral conversion and optical imaging [20–24]. For both experimental and theoretical analysis of the optical properties tuning the one of the most appealing systems are Cu-doped II-VI semiconductor QDs, as they can be prepared with a high degree of reproducibility and control, uniform shape and low polydispersity. The Cu ions in CdSe were shown to be able to act as a trap [25,26]. Although the copper related emission in CdSe has been observed earlier [27] it is still debated whether the Cu ions act as a trap for a hole or for the electron. The nature of the state associated with Cu impurities in core-shell II-VI nanocrystals was investigated in Ref. [28] by means of the spectroscopic and magneto-optical studies. It was demonstrated that in the nanocrystals under investigation the copper is incorporated as a magnetically active + 2 species and, hence, represents a source of optically active permanent holes. The presence of Cu ions in the II-VI QDs results in the long wavelength red-shifted emission with an effective Stokes shift about several hundreds of meV (given by the difference between the Cu ion acceptor level and the valence band edge energy) [18,28]. This allows to synthesize the Cu-doped QDs with an absorbtion

* Corresponding author.
E-mail address: vmantsev@gmail.com (V.N. Mantsevich).

https://doi.org/10.1016/j.jlumin.2019.05.001
Received 31 December 2018; Received in revised form 1 May 2019; Accepted 2 May 2019
Available online 08 May 2019

in the visible spectrum range and emission in the red and near infrared range of spectrum without reabsorption processes.

The origin of Cu dopant emission and the reasons for its high intensity, tunability, spectral width and non-linear optical properties are not yet well understood. Moreover, a careful analysis of excitons' behavior under the stationary excitation has not been performed previously, to the best of our knowledge, for the Cu-doped II-VI semiconductor QDs. In the present paper we report an experimental observation of PL and non-linear optical properties of the colloidal Cu-doped CdSe QDs. We have applied pump-probe technique for experimental analysis of exciton dynamics and non-linear optical properties investigation and also utilized a simple theoretical model for analysis of the experimental data and the estimation of exciton dynamics parameters. This paper is organized as follows: In Sec. 2 we describe the procedure of colloidal synthesis of Cu-doped CdSe QDs and their structure properties. Then in Sec. 3 we present the experimental setup and results. The latter are analyzed theoretically in Sec. 4. A comparison of theoretical predictions obtained from the simple rate equations model and experimental results allowed us to estimate parameters of exciton dynamics. Our main experimental and theoretical findings are summarized in concluding Sec. 5.

2. Synthesis and structural characterization of quantum dots

CdSe QDs capped with oleic ligands and doped with a different amount of copper were synthesized by the colloidal synthesis method described in Ref. [29]. The formation of tetrapod nanocrystals was previously performed by introducing organic ligands into the solution [30,31] or, alternatively, by using halides [32,33]. The thorough description of spherical QDs copper doping can be found in Ref. [16]. The advantage of our method is the ability to grow the copper-doped QDs with tetrapod shape. Our samples of CdSe QDs capped with oleic ligands and doped with a different amount of copper were synthesized by the colloidal synthesis method described in Refs. [34,35]. This technique differs from the method of spherical QDs growth in Ref. [36] by the addition of halides to provide the tetrapod formation and an extra copper doping. In a typical synthesis starting materials are cadmium acetate dihydrate $Cd(CH_3COO)_2{\cdot}2H_2O$ (analytical-grade), oleic acid (OA) $C_{17}H_{33}COOH$ (Aldrich, $90^0/_0$), selenium powder ($\geq$ 99, $99^0/_0$), diphenyl either Ph_2O (abcr, 99, $99^0/_0$), trioctylphosphine TOP (Aldrich, $97^0/_0$) and copper stearate (analytical-grade).

The synthesis starts from preparation of cadmium oleate solution 0.088 M (from cadmium acetate and oleic acid dissolved in diphenyl ether) and trioctylphosphine selenide (TOPSe) solution 1 M (obtained by dissolving selenium powder in TOP). The cadmium precursor solution (0.5 mmol) was then introduced into a flask together with 7 or 50 μmol of copper stearate. The obtained mixture was heated up to 200°C in Ar flow, and 0.45 mL of 1 M TOPSe solution in TOP was injected while stirring. After particles kept growing for 5 min the reaction system was cooled down to the room temperature. For the post-synthetic purification an equal amount of acetone (works as antisolvent) was added to the samples, resulting in the precipitation of QDs. The precipitated QDs were redispersed in hexane. Then, the QDs were again precipitated with acetone and once more dispersed in hexane to achieve a sufficient purity. The samples dispersed in hexane were stored in glass vials in the dark. Specimen designation and some important parameters of the samples are presented in Table 1.

Table 1
Specimen designation, content of Cu in synthesis/products and wavelengths of the basic exciton (electron-hole) transition [$1S_{3/2}(h) - 1S(e)$].

Sample	ν_{Cu}, μmol	at % Cu	λ, nm
CdSe(Cu)535	7	0.12	535
CdSe(Cu)552	50	0.52	552

ν_{Cu} is the amount of added Cu stearate. Quantitative elemental analysis was carried out on a ReSPECT energy-dispersive X-ray fluorescence (XRF) spectrometer using the selenium and copper $KL_{2,3}$ lines and a Fe internal standard. It was found that the number of Cu is 0.12 % and 0.52 % for $CdSe(Cu)535$ and $CdSe(Cu)552$ samples respectively. These values correspond to the average number of Cu dopants about 0.4 and 1.7 per nanocrystal [40].

Transmission electron microscopy (TEM) studies were performed using JEOL JEM 2100 microscope operating at 200 kV. TEM images were obtained by drop-casting QD/hexane sols on Cu carbon grids. X-ray diffraction (XRD) measurements were performed with the use of a Rigaku D/MAX 2500 diffractometer (Cu $K\alpha$ radiation, rotating anode, Bragg-Brentano scheme, graphite monochromator). Low-resolution transmission electron microscopy (TEM) images of copper doped CdSe QDs are shown in Fig. 1.

The morphology of the synthesized QDs depends on the amount of copper stearate added during synthesis procedure. The QDs exhibit an anisotropic shape and look like tetrapods. Sample $CdSe(Cu)535$ exhibits long legs with length 8 ± 2 nm and width 2.5 ± 0.5 nm. Contrary, the sample $CdSe(Cu)552$ reveals tetrapods with short legs with the length 4.5 ± 1 nm and the width similar to the $CdSe(Cu)535$ sample - 2.5 ± 0.5 nm. The length of tetrapod QDs legs does not influence the value of the basic exciton transition energy [41]. The energy of the basic exciton transition of tetrapod-shaped QDs is determined by the legs' thickness. Within the measured TEM resolution, the thickness of the legs for both samples is approximately the same (see Fig. 1). However, the measured spectra of linear absorption allow to conclude that average thickness of $CdSe(Cu)552$ QDs legs exceeds the thickness for $CdSe(Cu)535$ QDs legs by about $0.1 - 0.2$ nm.

The XRD pattern (see Fig. 2) of the samples demonstrates three main peaks at diffraction angles of $2\theta = 25.05^0$, 42.29^0 and 49.26^0 corresponding to (111), (220) and (311) planes of the cubic zinc blende (ZB) structure [37–39] (JCPDS file no. 19–0191). The XRD peaks reveal broad shape due to the small size of the QDs. The small shift from the database values in $CdSe(Cu)552$ diffraction peaks occurs due to the structure distortions of the QDs caused by the presence of copper ions.

3. Experimental results

For study of the linear and nonlinear optical properties of QDs at the room temperature we utilized the pump-probe technique (see Fig. 3). The pumping was performed by the mode-locked Nd^{3+}:$YAlO_3$ laser second harmonic (λ = 540 nm, pulse duration about 10 ns). As a probe we used a broadband PL radiation of the Coumarin-7 dye excited by the third harmonic (λ = 360 nm) of the pumping laser. The probe pulse duration was 11 ns, and we adjusted it to overlap with the pump pulse. Because of a relatively long pulse duration we probe the steady state of the system. The transmission and absorption of the probe light was measured with spectral resolution using SpectraPro 2300*i* spectrometer with PIXIS 256 CCD-camera. To obtain the correct nonlinear transmission and differential transmission spectra, we additionally measured the QDs' PL spectra for applied excitation intensities and subtracted these spectra from the coumarin PL spectra passing through the excited sample. The pump intensity tuning was done by means of the neutral optical filters. Dashed lines in Fig. 3 demonstrate part of the experimental setup utilized for the measurements of the colloidal QDs PL spectra as a function of pump intensity.

The absorption spectra of copper-doped CdSe QDs ($CdSe(Cu)535$ and $CdSe(Cu)552$) in 1 mm cell with hexane in the absence of pumping are shown in Fig. 4. The concentration of QDs dissolved in hexane was about 10^{17} cm^{-3}. The pronounced peak corresponds to the basic exciton transition ($1S_{3/2}(h) - 1S(e)$). The energy of this transition is determined by the size quantization effects in colloidal QDs. One can see that the peak shifts in $CdSe(Cu)535$ QDs with respect to $CdSe(Cu)552$ QDs due to the size quantization effects. The wavelength of the pump laser is shown by the green arrow in Fig. 4. This wavelength corresponds to the

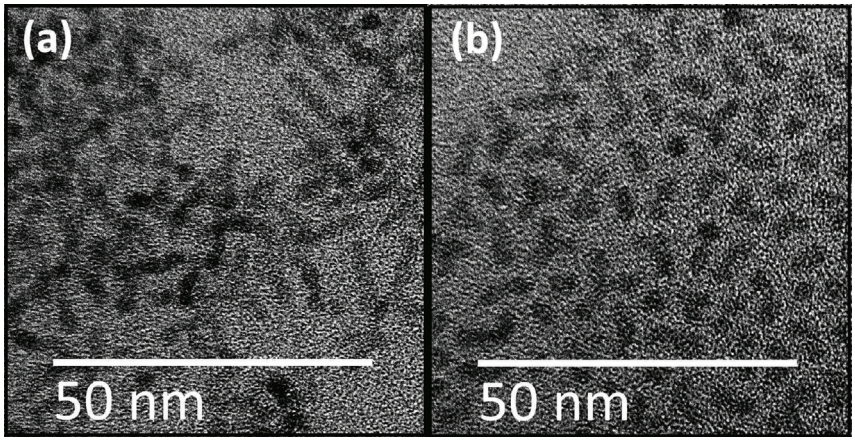

Fig. 1. Low-resolution transmission electron microscopy (TEM) images of synthesized copper-doped CdSe QDs (a) $CdSe(Cu)535$ and (b) $CdSe(Cu)552$.

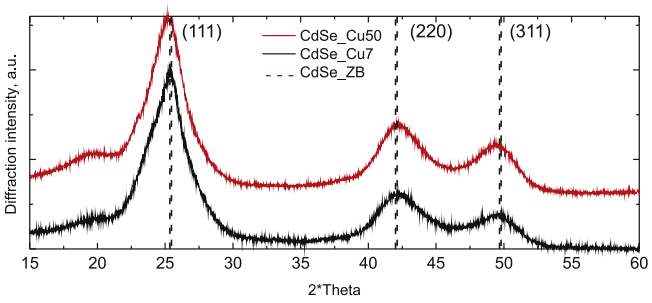

Fig. 2. X-ray diffraction of copper-doped CdSe QDs.

basic exciton transition in the $CdSe(Cu)535$ QDs. As a result the pump light resonantly excites the corresponding excitonic states in the $CdSe(Cu)535$ sample and non-resonant excitation occurs for the $CdSe(Cu)552$ QDs.

4. Explanation of experimental results by a kinetic model

The PL spectra of the copper-doped CdSe QDs for different pump powers are shown in Fig. 5. Pump intensities vary monotonically from 1 W/cm^2 for grey curves to 11 MW/cm^2 for black curves. For both samples PL spectra reveal a narrow luminescence peak with the full width at a half maximum (FWHM) about 40 nm associated with the basic excitonic transition and wide long-wavelength luminescence peak with FWHM about 250 nm caused by the presence of copper ions. For the QDs with higher concentration of Cu ions long-wavelength luminescence peak becomes more pronounced. Increase of the pump power leads to the growth of the PL intensity both for the peak attributed to the basic excitonic transition and for the peak caused by the presence of copper ions. For both samples the growth of pump intensity causes a fast saturation of Cu-associated PL (see Fig. 5) while saturation of PL

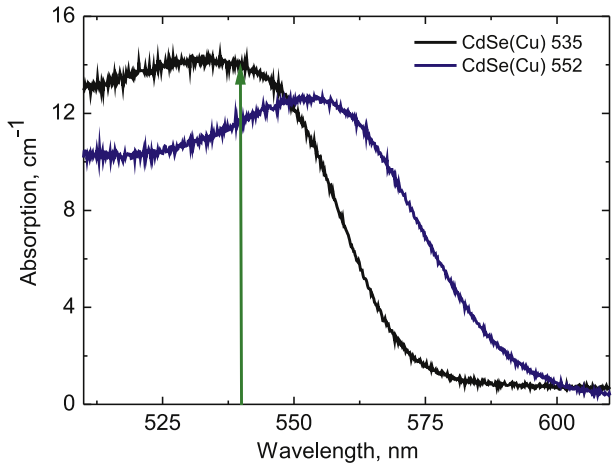

Fig. 4. Absorption spectra of colloidal solution of $CdSe(Cu)535$ and $CdSe(Cu)552$ QDs. Green arrow shows the pump laser wavelength. (For interpretation of the references to colour in this figure legend, the reader is referred to the Web version of this article.)

associated with the basic excitonic transition was not observed. In order to perform the detailed analysis we extract the areas under the PL peaks corresponding to the basic excitonic transition and Cu ions as a function of the pump power. The results are shown in Figs. 6 and 7a, where the saturation for Cu-associated PL and the absence of saturation for basic excitonic transition is more evident. The saturation value and the intensity of Cu-associated PL depends on the doping concentration of copper ions. The presence of fast saturation of Cu-associated PL is caused by the states filling effect of Cu acceptor levels and by the long radiative lifetimes of the Cu states. Saturation of Cu-associated PL occurs at the pump intensities about 0.3 kW/cm^2 for $CdSe(Cu)535$ sample

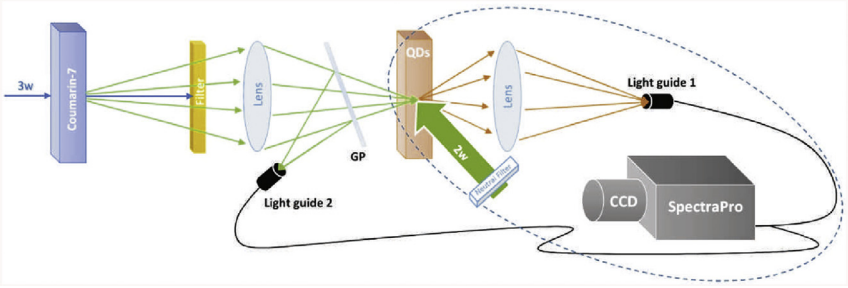

Fig. 3. Scheme of the experimental setup for quasi steady state pump-probe measurements. The probe light is delivered to the spectrometer combined with the CCD-camera (256 × 1024 matrix) by optical fibers.

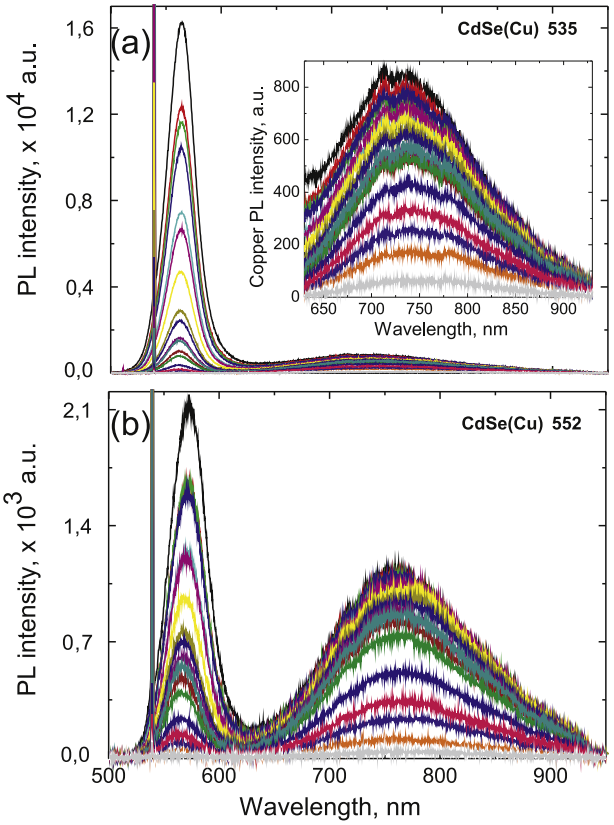

Fig. 5. Continuous PL spectra of (a) *CdSe(Cu)*535 and (b) *CdSe(Cu)*552 QDs for different pump intensities.

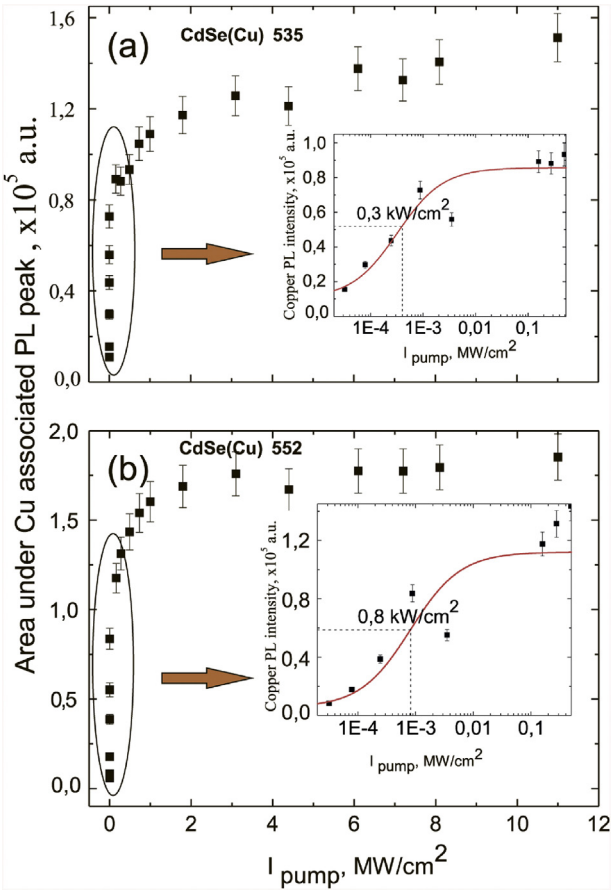

Fig. 6. Area under the copper-associated PL peak as a function of pump intensity for (a) *CdSe(Cu)*535 and (b) *CdSe(Cu)*552 QDs.

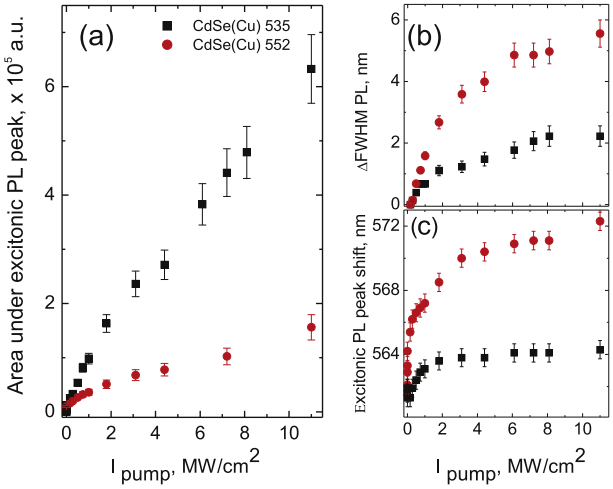

Fig. 7. (a) Area under the basic excitonic transition-associated PL peak (b) the broadening and (c) the shift as a function of pump intensity *CdSe(Cu)*535 and *CdSe(Cu)*552 QDs.

and at the pump intensities about 0.8 kW/cm^2 for *CdSe(Cu)*552 sample (see Fig. 6) which correspond to the absorption of a single photon per copper ion. This difference in intensity values is in accordance with the lower copper doping of *CdSe(Cu)*535 in comparison with *CdSe(Cu)*552. A copper-doped QD captures a single photon which excites an electron-hole pair. The hole is rapidly trapped [16] by the copper acceptor level with the typical lifetime about 300 − 500 nsec [43,44]. At the same time the linear dependence of the basic exciton PL on the pump intensity without any saturation effects can be seen (see Fig. 7a). Higher magnitudes of the PL for the *CdSe(Cu)*535 sample in comparison with the *CdSe(Cu)*552 sample arise due to the resonant excitation of the *CdSe(Cu)*535 **and lower Cu doping**. The FWHM was also analyzed as a function of pump intensity (see Fig. 7b). It was found that for both samples FWHM increases with the growth of excitation intensity. The FWHM broadening of the basic exciton PL up to 2 nm (8 meV) and 5.5 nm (22 meV) was revealed for resonantly **[***CdSe(Cu)*535**]** and non-resonantly *CdSe(Cu)*552 excited samples, respectively. We also found the long wave Stokes shift of the basic exciton PL for both samples (see Fig. 7c). Its value increases from 25 nm (98 meV) for the lowest excitation intensity to 29 nm (108 meV) for the highest excitation intensity in the case of resonant excitation and from 11 nm (42 meV) to 21 nm (79 meV) correspondingly for the non-resonant excitation.

The obtained values of PL broadening and PL red shift for the resonantly excited sample *CdSe(Cu)*535 are consistent with the effect of the increasing role of the biexciton PL with growth of the pump intensity [49–51]. In particular in Ref. [49] it was found that the red shift of biexcitons' binding energy with respect to excitons has been determined for individual NCs to be about 12 − 14 meV. The significantly higher values of PL broadening and PL red shift (33 meV) for the non-resonantly excited sample *CdSe(Cu)*552 compared with the resonant case (10 meV) can be explained by the coexistence of the biexciton PL increasing and reveal the fact that phonon-assisted absorption occurs [52]. The typical energy of LO-phonon in the QDs is about 25 meV ($\Delta\lambda$ 6 nm) [52–56] and corresponds well to our experimental results.

We should note that the temperature associated shift of the basic exciton spectrum in our case doesn't exceed 1 meV even in the case when all excitation energy is converted into the colloidal solution heating. We demonstrated earlier that for the pump intensities about 250 MW/cm^2 the exciton spectrum shift caused by the colloidal solution heating does not exceed 4 meV [45]. Thus, a colloidal solution heating could be excluded as a major reason of the spectrum shift. We associate

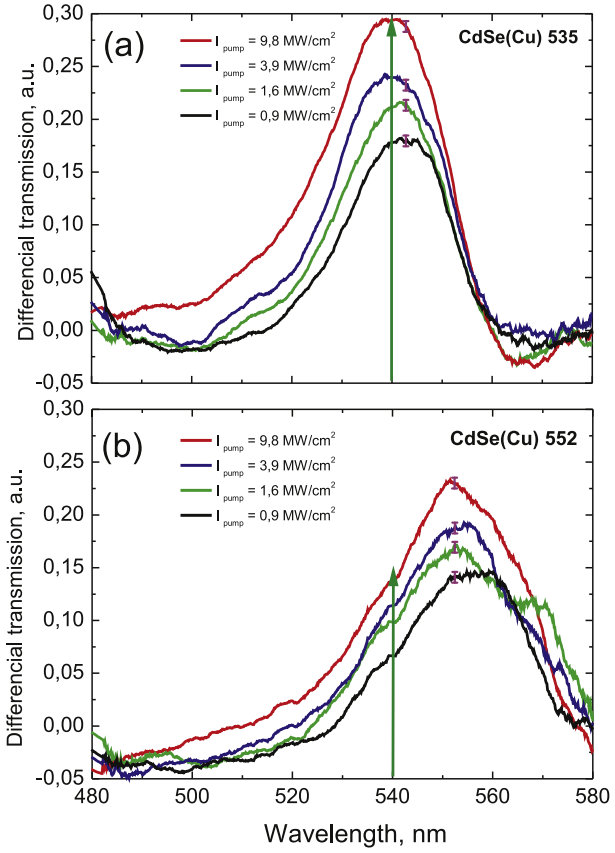

Fig. 8. The differential transmission spectra calculated from Eq. (1) for the different pump powers. Panel (a) corresponds to $CdSe(Cu)535$ QDs and panel (b) to $CdSe(Cu)552$ QDs. The vertical bars show the characteristic statistical errors. The green vertical arrow corresponds to the pump laser wavelength. (For interpretation of the references to colour in this figure legend, the reader is referred to the Web version of this article.)

long wavelength shift with an enhanced phonon-assisted absorption and recombination in Cu-doped CdSe QDs.

We also analyzed the behavior of nonlinear transmission spectra of colloidal Cu-doped CdSe QDs as a function of pump intensity both for resonant and non-resonant excitation. We introduce the differential transmission at a given wavelength λ as

$$DT(\lambda) = \frac{T_I(\lambda) - T_0(\lambda)}{T_0(\lambda)}, \tag{1}$$

where $T_I(\lambda)$ is the transmission of the solution of colloidal QDs under pumping with intensity I at the wavelength λ. The differential transmission spectra as a function of pump intensity for both samples are shown in Fig. 8. They directly reflect nonlinear optical properties of colloidal Cu-doped QDs and clearly reveal non-trivial exciton kinetics under nonlinear excitation. One could easily find significant changes in transmission at the wavelength of the basic exciton transition for both samples. The estimated number of exciting photons per single QD is about 100 at the maximum pump intensity (10 MW/cm^2). It means that nonlinear transmission behavior happens mostly due to the states filling effect. The obtained results demonstrate higher enlightenment of the **non-resonant** samples at the absorption maximum wavelength but not at the excitation wavelength **(see** Fig. 8b). It indicates the presence of strong electron-phonon interaction in the colloidal Cu-doped CdSe QDs.

The simultaneous linear growth of basic excitons PL (see Fig. 7a) and significant decrease of absorption at the basic exciton transition wavelength (see Fig. 8) with the pump intensity increasing can be explained by the growing influence of biexcitons formation on PL [49] and the presence of exciton-phonon interaction (exciton excitation accompanied by phonons [52]) and its strong influence on the PL and non-linear properties of Cu-doped colloidal CdSe QDs.

Non-resonantly excited QDs start to contribute to the absorption processes in the colloidal QDs solution with the growth of pump intensity. However, attenuation of PL and growth of non-radiative Auger processes' rates were not discovered despite the presence of excitons absorption saturation in the studied range of pump intensities [46–48]. The broadening of the basic exciton PL and its red shift with the increasing of pump intensity (see Fig. 7b and c) occur not only due to the growth of absorption but also due to the phonons accompanied radiation associated with QDs with lager diameters. We have analyzed the contribution of other mechanisms to nonlinearity, for example, trapped-carrier-induced Stark effect, discussed in Ref. [57]. It was shown that the spectral shift of absorption can be caused by an induced local electric field due to an electron or hole trapping at the QD's surface states, but this shift does not exceed 7 meV [45]. Charged excitons (negative or positive trions) also could be formed in nanocrystals. It was demonstrated that activation of Auger recombination of trion occurs as a result of thermal delocalization of one of the carriers from the CdSe core into the surface states, which can stimulate non-radiative Auger recombination with temperature increasing [61]. Thus, at room temperature trion levels are inactive for PL and does not influence the peak position and FWHM in the QDs PL spectrum. The analysis of fluorescence intermittency [62] revealed that QD with a single delocalized charge carrier (electron or hole) does not emit photons (“dark” QD). During the photon absorption the probability of nonradiative energy transfer from an exciton to a single charge is several orders of magnitude higher than exciton radiative recombination [63]. The latter effect results in PL attenuation and is characterized by a fast relaxation dynamics at the picosecond time scale. This is not consistent either with the PL intensity increasing with pump intensity growth or with absorption saturation of the basic exciton transition.

The properties of localized states formed by the Cu ions in the QDs are very important for understanding of the exciton recombination process. In order to describe the observed trend of PL behavior as a function of pump intensity we have developed a simplified rate equation model described below. The proposed model describes the behavior of photo-excited carriers in terms of populations of excitons (electron-hole pairs), i.e. for simplicity electrons and holes are not considered separately [42]. Fig. 9 illustrates the processes causing the light emission. The processes include optical excitation of excitons; light emission due to the recombination of electron-hole pairs corresponding to the basic exciton transition; relaxation with a characteristic time τ_{Cu} into the long-living states associated with the copper ions with a postponed emission of light. In the equations below we denote the exciton population for basic exciton transition and Cu states as N_{ex} and N_{Cu}, respectively. We also introduce notation $\tau_0^{ex(Cu)}$ for the average recombination time of excitons corresponding to basic exciton transition and Cu states. Under this assumption the occupancies of excitonic states in the QDs obey the following kinetic equations,

$$\frac{dN_{ex}}{dt} = G_{ex} - \frac{N_{ex}}{\tau_0^{ex}} - \frac{N_{ex}}{\tau_{Cu}},$$

$$\frac{dN_{Cu}}{dt} = G_{ex}^{Cu} - \frac{N_{Cu}}{\tau_0^{Cu}} \cdot \left(1 - \frac{N_{Cu}}{N_{Cu}^0}\right) + \frac{N_{ex}}{\tau_{Cu}}. \tag{2}$$

Here G_{ex} and G_{ex}^{Cu} are the corresponding generation rates determined by the generation wavelength and a factor $\left(1 - \frac{N_{Cu}}{N_{Cu}^0}\right)$ corresponds to the saturation of copper ions associated states. We will consider the case when $G_{ex}^{Cu} = 0$ and $G_{ex} = G$. The system of Eq. (2) can be solved in the steady state, when the time derivatives are absent on the left hand side of the equations. The exciton generation rate is given by

$$G_{ex} = \frac{P_S}{\hbar\omega_0} \frac{2\Gamma_0}{\Gamma}, \tag{3}$$

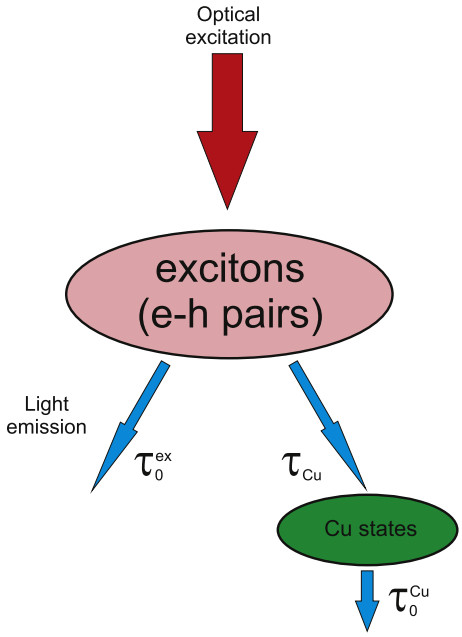

Fig. 9. The processes included in the theoretical model describing PL from the copper-doped CdSe QDs.

where ω_0 is the pump carrier frequency and $2\Gamma_0/\Gamma$ is the absorbance of the QD with Γ_0 and Γ being, correspondingly, radiative and non-radiative damping rates [64]. The radiative exciton damping rate is related to the radiative lifetime as $\tau_0 = 1/(2\Gamma_0)$. In the model case of an exciton in QW with infinitely high barriers one has [64].

$$\Gamma_0 = \frac{8e^2E_P}{n_b c a_B^2 \hbar\omega_0 m_0}, \tag{4}$$

where e is the electron charge, E_P is the interband momentum matrix element, n_b is the refractive index of the QD, c is the speed of light and m_0 is the free electron mass.

In order to compare the theoretical analysis with experimental results we assume that magnitude of PL peaks is proportional to the number of excitons. Under the assumption that the energy relaxation happens much faster than the exciton decay one has

$$\frac{N_{ex}}{N_{Cu}} = \frac{\tau_0^{Cu}}{\tau_0^{ex}}. \tag{5}$$

In the case of exciton saturation in the Cu associated states the density of excitons reads [65].

$$N_S = \frac{7}{8\pi a_B^2}, \tag{6}$$

where a_B is the 3D Bohr radius which is two times bigger than the excitonic Bohr radius in a narrow quantum well.

Using the following parameters for estimations, $\hbar\omega_0 = 2.2$ eV [66], $n_b = 2.3$, $a_B = 3.5$ nm [67] and $E_P = 23$ eV [68] we obtain $\hbar\Gamma_0 = 1.6$ eV which corresponds to radiative lifetime of an exciton at rest (with zero momentum). Considering a copper acceptor level with the typical lifetime about 400 nsec [43,44] one could compute a typical lifetime for the basic excitonic transitions which is about $\tau \sim 20$ ns.

5. Conclusions

This paper investigates PL properties and nonlinear transmission of Cu-doped CdSe colloidal QDs experimentally. We used the pump-probe technique with long pulse duration which allowed us to study the quasi steady state. A significant difference of the pump intensity dependent behavior of basic exciton transition and Cu dopants associated PL was found. We also studied experimentally the saturation of absorption in Cu-doped CdSe QDs and revealed the role of strong electron-phonon interaction in the PL properties and nonlinear transmission of colloidal Cu-doped CdSe QDs. The presence of exciton-phonon interaction and its strong influence on the PL and non-linear properties of Cu-doped colloidal CdSe QDs was proven by the simultaneous linear growth of basic exciton PL and substantial decrease of absorption at the basic exciton transition wavelength with the pump intensity increase. Our kinetic model allows to estimate the characteristic times for the basic exitonic transitions. We believe that investigation of nonlinear optical properties of copper-doped colloidal QDs performed in this paper will give a push to the development of optoelectronic devices capapble of operating at room temperature on the basis of colloidal QDs.

Acknowledgements

We acknowledge the support by the Russian Science Foundation (Project 18-72-10002).

References

[1] V.L. Colvin, M.C. Schlamp, A.P. Nlivisatos, Nature 370 (1994) 354.
[2] V.I. Klimov, A.A. Mikhailovsky, S. Xu, A. Malko, J.A. Hollingsworth, C.A. Leatherdale, H.J. Eisler, M.G. Bawendi, Science 290 (2000) 314.
[3] A.Y. Nazzal, L. Qu, X. Peng, M. Xiao, Nano Lett. 3 (2003) 819.
[4] J.F. Suyver, R. Bakker, A. Meijerink, J.J. Kelly, Phys. Status Solidi B 224 (2001) 307.
[5] J. Leeb, V. Gebhardt, G. Muller, D. Su, M. Giersig, G. McMahon, L. Spanhel, J. Phys. Chem. 103 (1999) 7839.
[6] R.N. Bhargava, D. Gallagher, X. Hong, A. Nurmikko, Phys. Rev. Lett. 72 (1994) 416.
[7] K. Sooklal, B.S. Cullum, S.M. Angel, C.J. Murphy, J. Phys. Chem. 100 (1996) 4551.
[8] D.J. Norris, N. Yao, F.T. Charnock, T.A. Kennedy, Nano Lett. 1 (2001) 3.
[9] V.A. Vlaskin, N. Janssen, J. van Rijssel, R. Beaulac, D.R. Gamelin, Nano Lett. 10 (2010) 3670.
[10] N. Pradhan, X.J. Peng, Am. Chem. Phys. 129 (2007) 3339.
[11] S. Jana, B.B. Srivastava, S. Acharya, P.K. Santra, N.R. Jana, D.D. Sarma, N. Pradhan, Chem. Commun. 46 (2010) 2853.
[12] A.A. Bol, J. Ferwerda, J.A. bergwerff, A. Meijerink, J. Lumin. 99 (2002) 325.
[13] S.C. Erwin, L. Zu, M.I. Haftel, A.L. Efros, T.A. Kennedy, D.J. Norris, Nature 436 (2005) 91.
[14] D.J. Norris, A.L. Efros, S.C. Erwin, Science 319 (2008) 1776.
[15] P.T.K. Chin, J.W. Stouwdam, R.A. Janssen, J. Nano Lett. 9 (2009) 745.
[16] K.E. Knowles, K.H. Hartstein, T.B. Kilburn, A. Marchioro, H.D. Nelson, P.J. Whitham, D.R. Gamelin, Chem. Rev. 116 (2016) 10820.
[17] J.F. Suyver, T. van der Beek, S.F. Wuister, J.J. Kelly, A. Meojerink, Appl. Phys. Lett. 79 (2001) 4222.
[18] G.K. Grandhi, R. Tomar, R. Viswanatha, ACS Nano 6 (2012) 9751.
[19] K. Nose, T. Omata, S. Otsuka-Yao-Matsuo, J. Phys. Chem. C 113 (2009) 3455.
[20] P. Wu, X.-P. Yan, Chem. Soc. Rev. 42 (2013) 5489.
[21] T. Jiang, J. Song, H. Wang, W. Zhang, M. Yang, R. Xia, L. Zhu, X. Xu, J. Mater. Chem. B 3 (2015) 2402.
[22] W. Zhang, Q. Lou, W. Ji, J. Zhao, X. Zhong, Chem. Mater. 26 (2014) 1204.
[23] L.R. Bradshaw, K.E. Knowles, S. McDowall, D.R. Gamelin, Nano Lett. 15 (2015) 1315.
[24] M. Sharma, K. Gungor, A. Yeltik, M. Olutas, B. Guzelturk, Y. Kelestemur, T. Erdem, S. Delikanli, J.R. McBride, H.V. Demir, Adv. Mater. 29 (2017) 1700821.
[25] I. Broser, H. Maier, H.J. Schulz, Phys. Rev. 140 (1965) 2135.
[26] A.L. Robinson, R.H. Bube, J. Appl. Phys. 42 (1971) 5280.
[27] P. Mandal, S.S. Talwar, S.S. Major, R.S. Srinivasa, J. Chem. Phys. 128 (2008) 114703.
[28] R. Viswanatha, S. Brovelli, A. Pandey, S.A. Crooker, V.I. Klimov, Nano Lett. 11 (2011) 4753.
[29] P.N. Tananaev, S.G. Dorofeev, R.B. Vasil'ev, T.A. Kuznetsova, Neorg. Mater. 45 (2009) 393.
[30] L. Manna, D.J. Milliron, A. Meisel, E.C. Scher, A.P. Alivisatos, Nat. Mater. 2 (2003) 382.
[31] L. Manna, E.C. Scher, A.P. Alivisatos, J. Am. Chem. Soc. 122 (2000) 12700.
[32] J. Lim, W.K. Bae, K.U. Park, L. Borg, R. Zentel, S. Lee, K. Char, Chem. Mater. 25 (2013) 1443.
[33] S. Ghosh, L. Manna, Chem. reviews 25 (2018) 1443.
[34] P.A. Kotin, S.S. Bubenov, T.A. Kuznetsova, S.G. Dorofeev, Mendeleev Commun. 25 (2015) 372.
[35] P.A. Kotin, S.S. Bubenov, N.E. Mordvinova, S.G. Dorofeev, Beilstein J. Nanotechnol. 8 (2017) 1156.
[36] R.B. Vasiliev, S.G. Dorofeev, D.N. Dirin, D.A. Belov, T.A. Kuznetsova, Mendeleev Commun. 14 (2004) 169.
[37] K.B. Subila, K.G. Kumar, S.M. Shivaprasad, K.G. Thomas, J. Phys. Chem. Lett. 2 (2013) 2774.
[38] Q. Pang, L. Zhao, Y. Cai, D.P. Nguyen, N. Regnault, N. Wang, S. Yang, W. Ge,

R. Ferreira, G. Bastard, J. Wang, Chem. Mater. 17 (21) (2005) 5263.
[39] N. Tam, N. Truong, T. Phuong, N. Nguyen, C. Park, Int. J. Photoenergy 2013 (2013) 146582.
[40] P.J. Whitham, K.E. Knowles, P.J. Reid, D.R. Gamelin, Nano Lett. 15 (2015) 4045.
[41] L. Zhao, Q. Pang, S. Yang, W. Ge, J. Wan, Phys. Lett. A 373 (2009) 2965.
[42] O. del Pozo-Zamundo, S. Schwarz, M. Sich, I.A. Akimov, M. Bayer, R.C. Schofield, E.A. Chekhovich, B.J. Robinson, N.D. Kay, O.V. Kolosov, A.I. Dmitriev, G.V. Lashkarev, D.N. Borisenko, N.N. Kolesnikov, A.I. Tartakovskii, 2D Mater. 2 (2015) 035010.
[43] Z.B. Siddique, Y. Yamamoto, T. Ohno, K. Nozaki, Norg. Chem. 42 (2003) 6366.
[44] K.E. Knowles, H.D. Nelson, T.B. Kilburn, D.R. Gamelin, J. Am. Chem. Soc. 137 (2015) 13138.
[45] A.M. Smirnov, A.D. Golinskaya, K.V. Ezhova, M.V. Kozlova, V.N. Mantsevich, V.S. Dneprovskii, J. Exp. Theor. Phys. Lett. 125 (2017) 890.
[46] D.I. Chepic, AlL. Efros, A.I. Ekimov, M.G. Ivanov, V.A. Kharchenko, I.A. Kudriavtsev, T.V. Yazeva, J. Lumin. 47 (1990) 113.
[47] V.A. Kharchenko, M. Rosen, J. Lumin. 70 (1996) 158.
[48] V.S. Dneprovskii, AlL. Efros, A.I. Ekimov, V.I. Klimov, I.A. Kudriavtsev, M.G. Novikov, Solid State Commun. 74 (1990) 557.
[49] Y. Louyer, L. Biadala, J.-B. Trebbia, M.J. Fernee, Ph Tamarat, B. Lounis, Nano Lett. 11 (2011) 4370.
[50] B. Patton, W. Langbein, U. Woggon, Phys. Rev. B 68 (2003) 125316.
[51] H.P. Wagner, H.-P. Tranitz, H. Preis, W. Langbein, K. Leosson, J.M. Hvam, Phys. Rev. B 60 (1999) 10640.
[52] A.M. Smirnov, A.D. Golinskaya, B.M. Saidzhonov, R.B. Vasiliev, V.N. Mantsevich, V.S. Dneprovskii, JETP Lett. (Engl. Transl.) 109 (2019) 370.
[53] D. Valerini, A. Creti, M. Lomascolo, L. Manna, R. Cingolani, M. Anni, Phys. Rev. B 71 (2005) 235409.
[54] F. Gindele, K. Hild, W. Langbein, U. Woggon, J. Lumin. 87–89 (2000) 381.
[55] S.A. Empedocles, D.J. Norris, M.G. Bawendi, Phys. Rev. Lett. 77 (1996) 3873.
[56] T.J. Liptay, L.F. Marshall, P.S. Rao, R.J. Ram, M.G. Bawendi, Phys. Rev. B 76 (2007) 155314.
[57] D.J. Norris, A. Sacra, C.B. Murray, M.G. Bawendi, Phys. Rev. Lett. 72 (1994) 2612.
[61] C. Javaux, B. Mahler, B. Dubertret, A. Shabaev, A.V. Rodina, Al L. Efros, D.R. Yakovlev, F. Liu, M. Bayer, G. Camps, L. Biadala, S. Buil, X. Quelin, J.-P. Hermieri, Nat. Nanotechnol. 8 (2013) 206.
[62] M. Nirmal, B.O. Dabbousi, M.G. Bawendi, J.J. Macklin, J.K. Trautman, T.D. Harris, L.E. Brus, Nature Nature 383 (1996) 802.
[63] M. Califano, A. Franceschetti, A. Sunger, Nano Lett. 5 (2005) 2360.
[64] E.L. Ivchenko, Optical Spectroscopy of Semiconductor Nanostructures, Alpha Science, Harrow UK, 2005.
[65] S. Schmitt-Rink, D.S. Chemla, D.A.B. Miller, Phys. Rev. B 32 (1985) 6601.
[66] R. Benchamekh, N.A. Gippius, J. Even, M.O. Nestoklon, J.-M. Jancu, S. Ithurria, B. Dubertret, Al L. Efros, P. Voisin, Phys. Rev. B 89 (2014) 035307.
[67] M.D. Tessier, C. Javaux, I. Maksimovic, V. Loriette, B. Dubertret, ACS Nano 6 (2012) 6751.
[68] S. Shokhovets, O. Ambacher, B.K. Meyer, G. Gobsch, Phys. Rev. B 78 (2008) 035207.